Research Square

Preprints are preliminary reports that have not undergone peer review.
They should not be considered conclusive, used to inform clinical practice,
or referenced by the media as validated information.

Phosphorus Release Kinetics from Native P-Starved Raphidocelis subcapitata: Interactions Between Up and Downstream Sediments and Wetland Soils

Hamed Arfania

h_arfania82@yahoo.com

University of Florida Everglades Research and Education Center

Jehangir Bhadha

University of Florida Everglades Research and Education Center

Research Article

Keywords: Phosphorous, release, soil, sediment, wetland

Posted Date: October 6th, 2025

DOI: https://doi.org/10.21203/rs.3.rs-7511899/v1

License: This work is licensed under a Creative Commons Attribution 4.0 International License.
Read Full License

Abstract

Quantifying phosphorus (P) release from wetland soils into overlying water is essential for predicting eutrophication risks. This study investigated the kinetics of P release from upstream and downstream river sediments and wetland soils and assessed its bioavailability using a standard algal (*Raphidocelis subcapitata*) assay. Rate parameters derived from the power function, parabolic diffusion, and Elovich models were strongly correlated with algal growth, highlighting the role of P in downstream and wetland eutrophication. The relationship between 0.5 M $NaHCO_3$-extractable P and algal growth increased from R^2 = 0.65 at the start to R^2 = 0.95 by the end of the experiment, while 0.5 M NaOH-extractable P showed strong correlations with kinetic model parameters. The two-site first-order kinetic model effectively described the trends in P release, revealing distinct mechanisms controlling P mobilization. High correlations (R^2 = 0.95) between algal growth and P bioavailability underscore the potential for eutrophication. The strong association between predicted P release and NaOH-extractable P suggests that moderately labile P pools play a key role in long-term nutrient availability. These findings demonstrate spatial variability in P release rates across sediments and wetland soils and emphasize the importance of wetland soils as potential long-term P sources. The continuous release of phosphorus from these soils may sustain or exacerbate eutrophic conditions, informing future nutrient management and wetland restoration efforts.

1. Introduction

Phosphorus (P) in river sediments is often regarded as a sink (Reddy and DeLaune, 2008; Kreiling et al., 2023); however, it can also serve as a source of P release (Ulrich and Köhler, 2011; Rodrigues et al., 2022), thereby influencing nutrient dynamics in aquatic ecosystems. P concentrations in freshwater systems link wetlands and lakes to the surrounding ecological environment. Due to the closed and fragile nature of these ecosystems, they are highly susceptible to changes in the Redfield Ratio (C:N:P = 106:16:1) of carbon, nitrogen, and phosphorus (Carey et al., 2019; Cheng et al., 2024). Therefore, maintaining the P balance in water is essential for sustaining life in wetland habitats. The release kinetics of P in sediments depends on the changes in pH, redox potential, and water temperature. The desorption of P from sediment into overlying water, often referred to as 'P release,' occurs over different timescales. It is relatively short in river systems due to continuous water flow, whereas in wetlands, the process is prolonged due to stagnant or slow-moving water. Therefore, phosphorus release from sediments is inherently a time-dependent process. These release dynamics are further governed by the hydrologic regime, which controls redox conditions, sediment-water interactions, and ultimately P fluxes in both restored and undisturbed wetlands (Aldous et al., 2005).

The Ramsar Convention, signed in 1971 in Ramsar, Iran, aims to conserve and promote the sustainable use of wetlands (WWF, 2023; Crocker et al., 2023). However, its implementation faces challenges from climate change and unsustainable resource management, particularly the overuse of soil and natural resources, which also impact local livelihoods. Nutrient management and animal husbandry, essential for agricultural productivity, significantly contribute to wetland eutrophication—a global issue driven by

excessive P (Smith et al., 1999). This P accumulation primarily results from the overapplication of fertilizers and erosion (Allen et al., 1993) and runoff from livestock production, including dairy and beef operations (Olivo et al., 2024; Bouwman et al., 2013). Wetlands retain phosphorus, which can initially support aquatic ecosystems and biodiversity (Mitsch & Gosselink, 2015). However, over time, sediment accumulation may lead to phosphorus release, as sediments function as internal P sources, potentially exacerbating downstream nutrient imbalances (Watson et al., 2016). To improve watershed management globally, addressing these challenges requires a deeper understanding of P release in wetland sediments. Guidance for setting nutrient criteria in wetland ecosystems emphasizes the need to integrate both biogeochemical processes and ecological responses (USEPA, 2008).

Various mechanisms, such as surface adsorption and the bioavailability of phosphorus, influence the release of phosphorus from river sediments and wetland soils (Kozyrev et al., 2023; Wiegman et al., 2024). Agricultural and livestock activities contribute to phosphorus imbalances in the watershed, often along with natural erosion processes (Olivo et al., 2024). Once sorption sites in wetland soil become saturated, they transition from nutrient sinks to sources of phosphorus release, exacerbating eutrophication (Turner and Newman., 2005). While algae can sometimes reduce pollution by assimilating phosphorus, their overgrowth, driven by excess nutrients, can worsen eutrophication (Paerl and Otten., 2013). Algae P-starved are effective bioindicators of phosphorus levels and algal bloom potential (Wei et al., 2023). The hypothesis is that upstream and downstream river sediments are in different equilibrium states regarding P release, with surface adsorption in the wetland reducing P bioavailability and making the wetland ecosystem less prone to eutrophic conditions than downstream sediments (Xu et al., 2024). However, continuous P release from wetland soils may still influence eutrophication. We propose that complex reactions, not just first- and second-order kinetics, govern the release of phosphorus (P) in river sediments and wetland soils. The validity of this hypothesis was tested using two-site second-order modeling and correlating P distribution and algal bioassays, providing insights into soil and sediment reactivity and ecosystem health.

2. Material and Methods

2.1. Study Area

The Kani Barazan Wetland, situated thirty kilometers northeast of Mohabad (Savojbolagh), is located between Mohabad Chai and Lake Urmia, at coordinates 36° 59' 23" N and 45° 45' 58" E (Fig. 1). This wetland is situated in the northern part of the Mohabad Chai drainage basin, extending north and east. The total area of the wetland is approximately 927 hectares. The maximum water depth reached 110 cm, while the minimum was 0.3 cm. However, during the wet season, the water depth can reach 120 cm, while it can fall to zero in dry periods.

Lake Urmia has experienced a significant decline in water levels over recent decades, which has altered the hydrology of the adjacent wetlands. During high-volume spring precipitation, water from the Kani Barazan Wetland flows into Lake Urmia through a single drainage channel located on the wetland's

eastern boundary. The average water depth in Lake Urmia has decreased by approximately 7–8 meters since the 1990s, which has affected the overall watershed hydrology. A drainage system on the northern side of the wetland prevents reverse flow from the lake to the wetland, protecting it from lake salinity. The wetland's water area covers approximately 463 hectares of the total 927 hectares, with portions of the area being dry during sampling periods. Mahabad's irrigation drainage network defines the boundary between wet and dry areas. The area exhibits acute mesotrophy in the spring, becomes eutrophic in the summer, returns to mesotrophy in the fall, and is oligotrophic in the winter. These fluctuations are primarily attributed to excessive fertilizer use in the upstream Mohabad Chai irrigation network (Fig. 2).

2.2. Sampling Procedure

Sampling was conducted in the rivers on the western side of Lake Urmia during the summer 2022. The sampling locations were identified using satellite imagery. Sediment samples were collected from the surface sediment at depths of 0–10 cm along the riverbanks. The sampling method involved selecting locations based on land use of the surrounding areas or potential pollution sources. Although the watersheds of the rivers are extensive, making systematic sampling challenging, efforts were made to collect samples from standard locations. During the summer season, river discharge in the province reaches its lowest levels, allowing for sediment collection. The collected samples were transferred to the laboratory, air-dried, and sieved through a 2-mm mesh for further analysis.

Sediment Analysis

All sediments and soils were air-dried, ground to pass a 2-mm screen, and analyzed for bicarbonate-extractable P (Olsen P; Olsen et al., 1954). The particle size distribution was determined using the method of Gee and Bauder (1986). In this method, a known mass of the samples was treated with a dispersing solution (sodium hexametaphosphate) after removing organic materials using hydrogen peroxide. The sample was passed through a 53-micron sieve to separate sand particles, and the particle size distribution of the particles that passed through the sieve was measured using a hydrometer at various time intervals, ranging from 10 to 30 seconds to 48 hours. The distribution of sand particle sizes was determined using a series of screens with mesh sizes of 1 mm, 0.5 mm, 0.25 mm, and 0.15 mm. The pH and electrical conductivity of the sediments in a 1:5 distilled water extract were measured using an electrical conductivity meter (Thomas, 1962). The calcium carbonate equivalent was determined using the back titration method with sodium hydroxide (Sims, 1996). Organic matter in the sediments was measured using the Walkley-Black method (Raul, 1994). Active calcium carbonate was calculated using the neutralization method with ammonium oxalate.

2.3. Phosphorus Fractionation

P fractions and potential bioavailability were evaluated using a modified Hedley sequential extraction. This procedure involves a series of extractions using solutions to enhance strength. Sediment samples were sequentially extracted using 1 M KCl, 0.5 M NaOH, 1 M HCl, and a 5:2 mixture of H_2SO_4 and HNO_3 in 50 mL polypropylene tubes (Hedley et al., 1982; Tiessen and Moir, 1993) Each sample was shaken for 8, 16, and 6 hours, respectively, and the extracts were separated via centrifugation. The ammonium

molybdate-ascorbic acid method was employed to determine the orthophosphate concentration in the extracts (Murphy and Riley, 1962).

2.4. Release Kinetics

1 gram of each soil sample was weighed in two replicates to investigate the kinetics of phosphorus release by sodium bicarbonate in the studied sediments. Then, 20 mL of 0.5 M sodium bicarbonate solution (pH 8.5) was added, maintaining a 1:20 sediment-to-extractant ratio. The mixture was shaken continuously at room temperature for durations of 5, 15, 30, 60, 120, 480, 600, 960, 1440, 2880, 2160, 5280, 8640, 11520, and 14400 minutes, a necessary condition for kinetic studies. At the end of each specified time, the suspension was filtered using filter paper. The orthophosphate concentration in the extracts was measured using a colorimetric method with a spectrophotometer at a wavelength of 880 nm.

The kinetic equations applied in this study included the first-order and second-order equations (Griffin and Jurinak, 1973), parabolic diffusion, and simplified Elovich models. Model fitting to the observed data was performed using linear regression, and the sum of squared errors was optimized using Excel software.

Ln (q_0-q) = a - b t First order

1/(q-q) = a + b t Second order

q = a + b t 0.5 Parabolic diffusion

Ln q = Ln a + b Ln t Power function

q = a + b Ln t Elovich

Where q_0 represents the amount of phosphorus released in 240 minutes, q is the phosphorus released at time t, and t is measured in hours. a and b are the constants of the equations. The first-order reactions of two sites, used by Santos et al. (2010) for phosphorus classification in two sections, are described by the following equation (Fangueiro et al., 2005):

$$q = \left(Q_1\left(1 - e^{-k_1 t}\right)\right) + \left(Q_2\left(1 - e^{-k_2 t}\right)\right)$$

Where q represents the amount of phosphorus released at time t, Q_1 (mg/kg) is the labile or easily accessible fraction with a release constant k_1, and Q_2 is the amount of phosphorus released from the medium labile or less exchangeable fraction, with a release constant k_2. The two sites in our model refer to (1) Q_1, representing readily bioavailable phosphorus that is easily accessible, and (2) Q_2, representing phosphorus that is slowly extractable by 0.5 M sodium bicarbonate. To compare the efficiency of the

models in predicting the phosphorus release rate from sediment samples, the coefficient of determination (r^2) and standard error (SE) were used, calculated with the following equations:

2.5. Algal Separation and Sediment Incubation

Samples were taken from the sediments of the Mohabad River at three points, approximately 10 meters apart. Two grams of dry sediment were cultured in 250 mL Erlenmeyer flasks with Guilard's medium (Guilard, 1975) and distilled water under continuous light (intensity of 4500 lux). Ten days later, the supernatant from the sediments was cultured on a solid medium in Petri dishes. The colonies were subcultured several times on agar plates to achieve 100% purity. The pure colonies of the species with morphological characteristics from the *Selenastraceae* family were then transferred to a liquid medium. The molecular analysis phase was initiated after cultivation and the accumulation of sufficient biomass. Molecular Identification Analysis: DNA was extracted from 0.1 g of pure microalgal biomass using the extraction and purification kit. After purity testing with a biophotometer, the DNA was used as a template for amplifying the ITS-2 region, which serves as the identification marker. The primers used were as follows: F: 5′-GCATCGATGAAGGCAGC-3′R: 5′-TCCTCCGCTTATTGATATGC-3′. The PCR program included an initial denaturation step at 94°C for 2 minutes, followed by 36 cycles of 94°C for 50 seconds, 62°C for 38 seconds, 72°C for 40 seconds, and finally, a 3-minute extension at 72°C. The PCR product was sequenced using the Sanger method after electrophoresis, and the amplified fragment was tested on a gel. The sequence results were BLASTed in the NCBI database. Algal-based assays are widely recognized for estimating bioavailable phosphorus and are often more reflective of ecological relevance than standard chemical extractions (Hegemann et al., 1983).

To conduct the study, phytoplankton cells were first isolated using a micropipette and cultured under standard conditions on a solid agar medium to facilitate their growth and proliferation. This medium provided suitable conditions for the initial development of microalgal colonies, and after several subcultures, they reached 100% purity. The purified colonies were then transferred to a liquid medium and cultured under appropriate conditions to obtain sufficient biomass for further molecular identification and analysis. The algal culture medium is prepared as follows. First, five stock solutions are prepared using chemical reagents from Merck. One milliliter of each stock solution is added to 900 milliliters of sterilized distilled water, and the total volume is adjusted to one liter. The pH of the medium is adjusted using 0.1 M NaOH and 0.1 M HCl. The culture medium should not be older than one week from the date of preparation (Fig. 4).

The algae were continuously cultured, extracted, and purified. The concentration of salts in the solution is as follows: 25.5 mg L^{-1} of $MgCl_2 \cdot 6H_2O$, 12.2 mg L^{-1} of $CaCl_2 \cdot 2H_2O$, 4.41 mg L^{-1} of $NaNO_3$, 14.7 mg L^{-1} of $MgSO_4 \cdot 7H_2O$, 1.04 mg L^{-1} of KH_2PO_4, and 15 mg L^{-1} of $NaHCO_3$. Additionally, the micronutrient salts include 185 mg L^{-1} of H_3BO_3, 416 mg L^{-1} of $MnCl_2 \cdot 4H_2O$, 3.27 mg L^{-1} of $ZnCl_2$, 1.43 mg L^{-1} of $CoCl_2 \cdot 6H_2O$, 0.01 mg L^{-1} of $CuCl_2 \cdot 2H_2O$, 7.26 mg L^{-1} of $Na_2MoO_4 \cdot 2H_2O$, 160 mg L^{-1} of $FeCl_3 \cdot 6H_2O$, and 300 mg L^{-1} of $Na_2EDTA \cdot 2H_2O$. They were grown under fluorescent and mercury vapor lamps with an intensity of 90 watts per square meter. During the growth stabilization phase, the algae were transferred to a

phosphorus-free culture medium and maintained for one month under these conditions until visible signs of phosphorus deficiency, such as an increase in size and rounding of the algae, became apparent. Visible signs of phosphorus deficiency, such as increased cell size and rounding, became apparent after one month of phosphorus starvation (Fig. 3). At this stage, 2 milliliters of a 5:1 sediment suspension to water, autoclaved for one hour, were added to 50 milliliters of phosphorus-free culture medium in 100-milliliter test tubes. The samples were regularly mixed twice a day. After one month, to compare algae growth in different samples, the number of algae was counted using a Thomas slide and a light microscope with 40× magnification (Fig. 4).

3. Results and Discussion

3.1. Physiochemical and Phosphorus Characteristics of River Sediments and Wetland Soils

Table 1 highlights key variations in the physiochemical properties and phosphorus distribution of river sediments and wetland soils. The upstream sediments (S1–S4) exhibited slightly alkaline pH values (7.2–7.7), with notable differences in electrical conductivity (EC) and calcium carbonate equivalent (CCE). The soil texture varied, with clay content ranging from 20% to 35% and sand content ranging from 12.5% to 45%. The downstream sediments (S5–S8) had consistent pH (7.2–7.5) and varied EC (0.3–1.06 dS m^{-1}), with the highest sand content observed in S5 (60%). The Kani Barazan Wetland soils (W1 and W2) showed significantly higher pH (7.8–8.1), EC (3.82–8.73 dS m^{-1}), and CCE (26%–41%), with soil texture containing significant clay content (35–37%), with the remainder composed of silt (50–52%) and sand (12.5%). Phosphorus availability was highest in the wetland soils, particularly for HCl-P in W2 (769 mg P kg^{-1}), and varied across the river sediments, with S2 showing the highest KCl-P concentration. These findings indicate that wetland soils have the highest phosphorus availability, whereas the river sediments exhibit greater variability in nutrient distribution.

Table 1
Physiochemical characteristics of soils from the Mohabad Chai upstream (S1–S4), downstream (S5–S8), and Kani Barazan Wetland (W1–W2), including phosphorus distribution in different fractions (KCl-P, NaOH-P, HCl-P). The table presents variations in pH, electrical conductivity (EC), calcium carbonate equivalent (CCE), active calcium carbonate equivalent (ACCE), soil texture (clay and sand content), and phosphorus availability across the sampling locations.

Labels		pH	EC	CCE	ACCE	Clay	Sand	KCl-P	NaOH-P	HCl-P
			$dS\ m^{-1}$	%				$mg\ P\ kg^{-1}$		
S1	Up	7.3	0.57	12	2.42	20	12	3.51	53.3	440
S2	Up	7.5	0.56	18	2.25	17	45	6.98	53.3	500
S3	Up	7.7	0.32	12	2.93	35	15	4.20	56.7	247
S4	Up	7.2	1.21	11	1.75	12	2.5	25	21.5	148
S5	Down	7.2	0.83	5	1.73	27	60	10.1	118	465
S6	Down	7.2	0.95	9	2.72	32	7	5.93	201.2	455
S7	Down	7.2	1.06	13	2.24	17	17	2.11	117.4	388
S8	Down	7.5	0.3	23	2.8	50	50	12.1	10.8	478
W1		8.1	3.82	26	3.79	37	12.5	5.9	16.2	582
W2		7.8	8.73	41	4.81	35	12.5	3.8	9.86	769

3.2. Release of P from soils and sediments

The graph of released phosphorus versus time for different sediments is shown in Fig. 5. Generally, phosphorus release from sediments occurs in an initial rapid reaction, followed by a slower reaction over time. In almost all of them, the release of P continues even after 24 hours; however, we reach equilibrium after some time, typically before 240 hours. However, most samples approached a pseudo-equilibrium in mid-term durations (24 to 48 hours). Equilibrium was defined as the reduction in the difference between the two final concentrations to less than 10%. Under these conditions, upstream river sediments reach equilibrium in the mid-term (24 hours). However, the downstream sediments and wetland soils remained pseudo-stable, and their release continued into the long term (88 to 240 hours) (Fig. 5).

The results from the BLAST analysis and phylogenetic tree construction showed a significant similarity with members of the *Selenastraceae* family for this species (Fig. 6). Different molecular markers, such as 18S, ITS, and rbcL, are widely used to identify genera and species in various organisms. The ITS marker is particularly effective due to its high copy number in the genome and its conserved sequences, making it suitable for identifying fungal species and chlorophyte algae (Nilsson et al., 2009; Alvarado et al., 2020). In this study, the ITS marker was employed for identification purposes. Members of the *Selenastraceae* family are susceptible to the concentration of pollutants and various elements, especially phosphorus. In 2003, Kamaya et al. examined the effect of different phosphorus

concentrations on the sensitivity of algae to other chemical elements. They concluded that, depending on the element type and the phosphorus deficiency range, the algae's sensitivity to toxicity increases (Kamaya et al., 2003). The molecular identity was confirmed through ITS2 sequencing, showing the characteristic crescent-shaped cells of Raphidocelis subcapitata (Fig. 6).

ITS2 Sequence:

CATTCGGAGGGACGATTGCAGAATTCCGTGATCATCGAATCTTTGAACGCACATTGC
GCCCCTGGCTATTCCAGGGAGCATGTCTGCCTCAGCGTCGTTTCACTCCTAACACTCT
GCCCTTGATGTGCGACAAGCTTTCCTGGTAACTTGATGTTGATGTGGCTTCCATTATC
GGCCTCTTTTCTGATTGGGTTGGATGAAGTTGAGAGGCTTGAGCAAGGACCCGTTAT
GGGCATCAACTGGATAGGTAGTGTCGGCCAACCTTGGTCGCTTACACGAAGTTGTTG
CTTGTGGACCTTGCTGGGGGCCAGCAGGAAACACGCTCACGCGTGATCTAAACCTTC
GACCTGGAGCTCAGGCAAGAACACCCGCTGAACTTAAGCATATCAATAAGCGGAGG
A

In this study, a native and climate-adapted species, Raphidocelis subcapitata, was identified and introduced through morphological and molecular analysis using the ITS2 marker. This species, a suitable bioindicator, is proposed for estimating bioavailable phosphorus and trophic status in rivers and wetlands within the Lake Urmia watershed. The relationship between the phosphorus released by the sodium bicarbonate solution and the growth of *Raphidocelis subcapitata* at different times is illustrated in Fig. 7. The results revealed a correlation between algal growth and phosphorus release, with a coefficient of determination (R^2) ranging from 0.65 to 0.85 in the initial hours, which increased to 0.95 by the end of the release period. This suggests that prolonged phosphorus release created more favorable conditions for algae growth. The Olsen phosphorus test, which extracts phosphorus over a short duration, may underestimate the bioavailable phosphorus for algae in sediments compared to its actual amount.

3.3. Comparison of Kinetic equations

The results of fitting kinetic equations to the observed phosphorus release data in the studied sediments are presented in Table 2. For phosphorus, comparing the coefficient of determination (r^2) and the standard error of estimation (SE) showed that the power function equation had the highest coefficient of determination and the lowest standard error for most sediments. This indicates that the power function equation is the most capable of describing the phosphorus release rate. However, the generally good fit of the power function equation may be due to the logarithmic transformation, which minimizes data sensitivity (Chen et al., 2015). Similar observations have been made in studies investigating the effects of various biotic and abiotic factors on phosphorus release from sediments, where bioturbation and redox processes have been shown to influence phosphorus availability (Chen et al., 2016).

The simplified Elovich equation satisfactorily explained the kinetics of phosphorus release in the sediments (Table 2). According to Hingston (1980), the Elovich equation can describe the desorption phenomenon in soils where a wide range of activation energies exist due to the complex nature of the

adsorption surfaces. However, caution is needed when drawing such conclusions, as the linear plot of phosphorus release against $t^{1/2}$ showed that the parabolic diffusion equation could not adequately describe phosphorus release. The mismatch between the parabolic diffusion equation and the observed data suggests that diffusion does not control phosphorus release. The zero-order, first-order, and second-order equations for all sediments could not describe phosphorus release by 0.5 M NaOH due to their low r^2 and high SE values.

For downstream samples (S1-S4), the Power Function model consistently provided the best fit, with high r^2 values (ranging from 0.71 to 0.97) and relatively low standard errors (SEs), particularly for S1, S3, and S4. In contrast, for samples S5-S8, the Parabolic model generally performed better, yielding r^2 values ranging from 0.68 to 0.94, but with higher standard errors (SEs) for some samples (e.g., S8). Among the wetland samples, W1 and W2, the Power Function model also showed the best fit, particularly for W2, where r^2 reached 0.94 with a low SE of 3.18, while W1 had a slightly lower fit with r^2 at 0.85 and a higher SE of 3.24. The Power Function model is the most suitable for modeling phosphorus release in the wetland and downstream sites, except for specific samples (S5-S8) where the Parabolic model is more fitting.

Table 2
Kinetic model fitting of phosphorus release from upstream and downstream of Mohabad Chai and Kanibarazan wetlands (S2, S3, S15, S25, etc.) using the First-Order, Second-Order, Power Function, Elovich, and Parabolic models. The table displays the coefficient of determination ($r2$) and standard error (SE) values for each model, providing insights into the model's accuracy and suitability for the respective samples. Higher $r2$ values and lower SE indicate a better fit for the given data.

	First Order		Second Order		Power Function		Elovich		Parabolic	
	r^2	SE	r^2	SE	r^2	SE	r^2	SE	r^2	SE
S1	0.91	0.07	0.95	339	0.97	0.07	0.99	1.25	0.84	4.22
S2	0.74	0.55	0.79	279	0.71	0.36	0.91	6.82	0.53	1.95
S3	0.63	0.36	0.81	313	0.92	0.13	0.96	2.8	0.67	7.43
S4	0.7	0.28	0.81	350	0.73	0.24	0.9	3.85	0.55	8.26
S5	0.75	0.1	0.81	111	0.95	0.14	0.98	7.22	0.82	2.14
S6	0.75	0.15	0.71	130	0.93	0.13	0.97	6.81	0.75	21.2
S7	0.87	0.18	0.93	190	0.89	0.13	0.98	3	0.68	12.08
S8	0.76	0.25	0.9	140	0.94	0.54	0.96	7.22	0.68	21.3
W1	0.53	0.43	0.75	332	0.85	0.18	0.94	3.24	0.6	8.83
W2	0.86	0.07	0.94	166	0.88	0.16	0.97	3.18	0.81	8.81

The zero-order, first-order, and second-order equations in all sediment samples were unable to describe phosphorus release using 0.5 M sodium bicarbonate, as indicated by their low r^2 values and high standard error (SE) values. Despite the low coefficient of determination for the first-order and second-order equations, fitting them to the short-term data (16 hours) significantly increased their r^2 values. This indicates that the phosphorus release rate in the short term follows a different mechanism or that the apparent rate constantly changes over time. The phosphorus release curve consisted of an initial curved-linear segment and a second flat-linear segment. Separating the phosphorus release curve into these two linear parts significantly improved the coefficient of determination. Furthermore, this separation allowed the calculation of phosphorus release rates at different time intervals.

3.4. Two-Site First-Order Model

As a result, the two-site first-order model was fitted to the observed data and successfully predicted the phosphorus release trend (Table 3). The model variables were obtained from nonlinear fitting, along with the coefficient of determination. The two-site first-order model accurately described the phosphorus release kinetics in all sediment samples. Applying this model to the present study data revealed two main components: Q_1, which represents the readily bioavailable phosphorus that is easily accessible. Q_2: Represents phosphorus that is slowly extractable by 0.5 M sodium bicarbonate. The range of Q_1 fluctuated between 17.01 and 61.3 mg kg-1, with an average of 40.8 mg kg-1, while Q_2 ranged from 13.5 to 82.8 mg kg^{-1}, with an average of 46.8 mg kg^{-1}. In general, the release rate coefficient (k_1) for the initial phase (readily bioavailable phosphorus) was higher than that for the second, slower phase (k_2). The mean values were $k_1 = 6.07\ h^{-1}$ and $k_2 = 0.08\ h^{-1}$. This difference indicates the retention of phosphorus in two distinct locations. The bicarbonate ion facilitates the extraction of bioavailable phosphorus from sediments through three mechanisms: Cation hydrolysis, Anion exchange, and Cationic complexation.

Table 3
First-order kinetic model for phosphorus release from upstream and downstream sediment of Mohabad River and Kani Brazan Wetland. The data shows both sites' release rate constants (k1) and equilibrium concentrations (Q1), illustrating the differences in phosphorus release dynamics between the river and wetland sediments. The model's high $r2$ values indicate a strong fit, highlighting the temporal variation in phosphorus release from different environments and the potential impact on water quality and eutrophication processes in the region.

	Q_1	k_1	Q_2	k_2	SE	r^2	Q_1/Q_2
S1	19.9	4.92	20.9	0.03	1.52	0.99	0.94
S2	39.5	3.94	38.3	0.15	2.52	0.99	1.03
S3	17.01	6.85	26.02	0.1	1.46	0.99	0.65
S4	36.06	3.26	13.5	0.05	1.54	0.99	2.59
S5	61.3	2.71	109	0.04	8.76	0.99	0.56
S6	57.9	4.56	81.1	0.07	8.52	0.99	0.71
S7	49.9	4.75	35	0.06	2.91	0.99	1.42
S8	56.2	18.9	82.8	0.13	5.39	0.99	0.67
W1	25.5	6.63	26	0.11	1.31	0.99	0.98
W2	45.5	35.6	35.6	0.02	2.57	0.99	1.27

3.5. Correlations and implications for environmental health

Algal growth exhibits strong positive correlations (0.92–0.95) under the Parabolic Diffusion, Simplified Elovich, and Power Function models, indicating significant relationships with soil and phosphorus properties. Phosphorus fractions, such as NaOH-P and KCl-P, exhibit moderately strong positive correlations across these models. In contrast, the Second-order model demonstrates notable negative correlations, particularly with algal growth (-0.74 to -0.86) and NaOH-P (-0.69 to -0.57). Soil properties, such as pH, clay, and sand, exhibit variable trends depending on the model; for example, the Power Function model shows stronger correlations with sand, while the First-order model exhibits weak positive correlations with pH and electrical conductivity (EC). These observations emphasize the importance of selecting appropriate kinetic models to understand the relationships between soil properties, phosphorus fractions, and algal growth. These patterns may be further exacerbated by climate-driven shifts in hydrology and redox processes, which are known to influence phosphorus and nitrogen mobility and legacy release in wetlands (Jarvie et al., 2020).

A two-site second-order kinetic model was employed to assess the release of P from river sediments and wetland soil over time. Our analysis revealed that wetland soils exhibited a more prolonged P release than river sediments, which showed rapid initial release followed by decreased release rates.

This suggests that while wetland soils function as temporary nutrient sinks, they can transition into nutrient sources under certain conditions as P sorption sites become saturated (Turner and Newman, 2005). In contrast, the river sediments showed an initial burst of P release, followed by a more stable phase.

Algal bioassays were used to assess the bioavailability of P. We observed higher P bioavailability in river sediments, as indicated by the elevated algal growth in these environments. This supports the hypothesis that the bioavailability of P in river sediments is higher due to less surface adsorption than wetland soils. Algae, a well-known indicator of eutrophic conditions, further confirmed that excess nutrient loading could lead to harmful algal blooms in river ecosystems.

The results suggest that the equilibrium states of P release differ between upstream and downstream sediments. In river sediments, where surface adsorption is less dominant, phosphorus is more readily available for biological uptake, increasing the potential for eutrophication, especially in nutrient-rich conditions. Conversely, due to their ability to absorb phosphorus, wetland soils function as a less bioavailable source of P, which could help mitigate eutrophication in the short term. However, as wetland soils transition from being nutrient sinks to sources, they continue to contribute to long-term nutrient cycling. They can exacerbate eutrophication under certain conditions, particularly when sorption sites become saturated. Despite their initial role as nutrient sinks, the continuous release of P from wetland soils could still have significant implications for water quality and ecosystem health. This dynamic, coupled with the findings from the two-site second-order modeling and algal bioassays, provides a more comprehensive understanding of P dynamics in river and wetland ecosystems.

Conclusion

Our findings support the hypothesis that the phosphorus release mechanisms in river sediments and wetland soils are influenced by surface adsorption and bioavailability, with implications for eutrophication potential and overall ecosystem health. These insights are critical for managing phosphorus loading in regions such as the Lake Urmia watershed, where nutrient cycling and water quality are of utmost concern. This study provides valuable insights into the differences in phosphorus availability and release dynamics between river sediments and wetland soils, with significant implications for environmental quality, ecological health, and human health. The findings suggest that wetland soils have higher phosphorus availability and contribute to prolonged phosphorus release, which can influence eutrophication potential. The two-site first-order model effectively captured the release kinetics, enhancing our understanding of phosphorus dynamics in these environments. These results are crucial for managing nutrient cycling in river and wetland ecosystems, particularly in regions such as the Lake Urmia watershed, where phosphorus is a critical factor in water quality. Particularly, legacy phosphorus stored in wetland soils may be slowly released over extended periods, maintaining eutrophic conditions long after external loading has ceased (Nair et al., 2015). Effective phosphorus management in these ecosystems is essential to prevent eutrophication, protect biodiversity, and ensure the sustainability of freshwater resources vital for ecological health and human populations.

Statements and Declarations

Competing Interests

The authors have no relevant financial or non-financial interests to disclose

Data Availability

The datasets generated during and/or analyzed during the current study are available from the corresponding author on reasonable request.

Author Contributions

Hamed Arfania contributed to the study conception and design, material preparation, data collection and analysis, and wrote the first draft of the manuscript. Jehangir Bhadha contributed to the study design and manuscript review. Both authors commented on previous versions of the manuscript. All authors read and approved of the final manuscript.

References

1. Aldous, A., McCormick, P., Ferguson, C., Graham, S., and Craft, C. (2005). Hydrologic regime controls soil phosphorus fluxes in restoration and undisturbed wetlands. Restoration Ecology, 13, 341–347. https://doi.org/10.1111/j.1526-100X.2005.00043.x
2. Allan, C.J., Roulet, N.T. and Hill, A.R. (1993). The biogeochemistry of pristine, headwater Precambrian shield watersheds: an analysis of material transport within a heterogeneous landscape. *Biogeochemistry*, 22, 37-79.
3. Alvarado, A., Tello, M. A., & Cruz, M. (2020). Molecular markers in algal biodiversity and their application in environmental monitoring. *Environmental Science and Pollution Research*, 27(2), 1961-1971. https://doi.org/10.1007/s11356-019-06843-2
4. Arfania, H., Samadi, A., Asadzadeh, F., Sepehr, E. and van der Zee, S., 2022. Implications of Sediment Properties on Phosphorus Availability to the Selenastrum capricornutum in Urmia Lake Rivers. CLEAN–Soil, Air, Water, 50(8), p.2200164. https://doi.org/10.1002/clen.202200164
5. Barrow, N.J. (1983). A mechanistic model for describing the sorption and desorption of phosphate by soil. *Journal of Soil Science*, 34(4), 733-750.
6. Bouwman, L., Goldewijk, K.K., Van Der Hoek, K.W., Beusen, A.H., Van Vuuren, D.P., Willems, J., Rufino, M.C. and Stehfest, E. (2013). Exploring global changes in nitrogen and phosphorus cycles in agriculture induced by livestock production over the 1900–2050 period. *Proceedings of the National Academy of Sciences*, 110(52), 20882-20887.
7. Carey, J.C., Jankowski, K., Julian, P., Sethna, L.R., Thomas, P.K. and Rohweder, J. (2019). Exploring silica stoichiometry on a large floodplain riverscape. *Frontiers in Ecology and Evolution*, 7, 346.
8. Chen, M., Ding, S., Liu, L., Xu, D., Gong, M., Tang, H., & Zhang, C. (2015). Kinetics of phosphorus release from sediments and its relationship with arsenic adsorption during sediment resuspension. *Science of the Total Environment*, 536, 55-62. https://doi.org/10.1016/j.scitotenv.2015.10.155

9. Chen, M., Ding, S., Liu, L., Xu, D., Gong, M., Tang, H., & Zhang, C. (2016). Kinetics of phosphorus release from sediments and its relationship with iron speciation influenced by the mussel (Corbicula fluminea) bioturbation. *Science of the Total Environment*, 568, 573-582. https://doi.org/10.1016/j.scitotenv.2015.10.155
10. Cheng, J., Qin, L., Kong, L., Tian, W. and Zhao, C. (2024). Temporal variation of soil phosphorus fractions and nutrient stoichiometry during wetland restoration: implications for phosphorus management. *Environmental Research*, 120486.
11. Crocker, R., Blake, W.H., Hutchinson, T.H. and Comber, S. (2023). Aquatic phosphorus behaviour within a UK Ramsar wetland: Impacts of seasonality and hydrology on algal growth and implications for management. *Science of The Total Environment*, 893, 164606.
12. Fangueiro, D., van der Zee, S.E.A.T.M., & Cabral, F. (2005). Phosphorus release from dairy manure derived materials: Water extraction kinetics and sequential fractionation. *Journal of Environmental Quality*, 34(3), 1058-1066. https://doi.org/10.2134/jeq2004.0353
13. Gee, G.W., & Bauder, J.W. (1986). Particle-size analysis. In A. Klute (Ed.), *Methods of Soil Analysis, Part 1: Physical and Mineralogical Methods* (2nd ed., pp. 383-411). American Society of Agronomy. https://doi.org/10.2136/sssabookser5.1.2ed.c15
14. Griffin, R.A., & Jurinak, J.J. (1973). Estimation of activity coefficients from the electrical conductivity of natural solutions. *Soil Science*, 116(1), 26-30. https://doi.org/10.1097/00010694-197307000-00006
15. Guillard, R.R.L. (1975). Culture of phytoplankton for feeding marine invertebrates. In W.L. Smith & M.H. Chanley (Eds.), *Culture of Marine Invertebrate Animals* (pp. 29-60). Springer US. https://doi.org/10.1007/978-1-4615-8714-9_3
16. Hegemann, D.A., Johnson, A.H., and Keenan, J.D. (1983). Determination of algal-available phosphorus on soil and sediment: A review and analysis. Journal of Environmental Quality, 12, 12–16. https://doi.org/10.2134/jeq1983.00472425001200010000
17. Hedley, M. J., Stewart, J. W. B., & Chauhan, B. S. (1982). The effects of fertilization and cropping on phosphorus fractions in soils of different textures. Soil Science Society of America Journal, 46(5), 798-803.
18. Hingston, F.J. (1980). Adsorption and desorption of ionic species on surfaces of minerals and soils. *Journal of Soil Science*, 31(4), 615-627. https://doi.org/10.1111/j.1365-2389.1980.tb02750.x.
19. Jarvie, H.P., Pallett, D.W., Schäfer, S.M., Clarke, M., Jones, A., Bowes, M.J., and Scarlett, P. (2020). Biogeochemical and climate drivers of wetland phosphorus and nitrogen release: Implications for nutrient legacies and eutrophication risk. Journal of Environmental Quality, 49, 1703–1716. https://doi.org/10.1002/jeq2.20155
20. Kamaya, N., Yamamoto, Y., & Nakano, T. (2003). Effects of phosphorus on the sensitivity of algae to other chemical elements in aquatic ecosystems. *Ecological Engineering*, 19(1), 34-41. https://doi.org/10.1016/S0925-8574(02)00148-5

21. Kuo, S. (1996). Phosphorus. In D.L. Sparks (Ed.), *Methods of Soil Analysis, Part 3: Chemical Methods* (pp. 869-919). Soil Science Society of America, American Society of Agronomy. https://doi.org/10.2136/sssabookser5.3.c32
22. Kozyrev, R., Umezawa, Y. and Yoh, M. (2023). Total phosphorus and phosphorus forms change in sediments along the Tone River. *Frontiers in Earth Science*, 11, 1060312.
23. Kreiling, R.M., Anderson, E.B., & Fennessy, M.S. (2023). Phosphorus retention and release in streambed sediment in a western Lake Erie watershed. *Science of the Total Environment*, 848, 157662. https://doi.org/10.1016/j.scitotenv.2022.157662
24. Mitsch, W.J., & Gosselink, J.G. (2015). *Wetlands* (5th ed.). John Wiley & Sons.
25. Murphy, J., & Riley, J.P. (1964). A modified single solution method for the determination of phosphate in natural waters. *Analytica Chimica Acta*, 27, 31-36. https://doi.org/10.1016/S0003-2670(00)88444-5
26. Nair, V.D., Clark, M.W., and Reddy, K.R. (2015). Evaluation of legacy phosphorus storage and release from wetland soils. Journal of Environmental Quality, 44(6), 1956–1964. https://doi.org/10.2134/jeq2015.03.0154
27. Nilsson, R.H., Tedersoo, L., Lindahl, B.D., et al. (2009). The ITS region is a tool for exploring the fungal diversity of soils. *Fungal Diversity*, 39(1), 1-12. https://doi.org/10.1007/s13225-009-0026-7
28. Paerl, H.W. and Otten, T.G. (2013). Harmful cyanobacterial blooms: causes, consequences, and controls. *Microbial Ecology*, 65, 995-1010.
29. Paytan, A. and McLaughlin, K. (2012). Tracing the sources and biogeochemical cycling of phosphorus in aquatic systems using isotopes of oxygen in phosphate. In *Handbook of Environmental Isotope Geochemistry: Vol I*, 419-436.
30. Raul, P. (1994). Determination of organic matter using the Walkley-Black method. *Soil and Plant Analysis Manual* (3rd ed.).
31. Reddy, K.R., & DeLaune, R.D. (2008). Phosphorus biogeochemistry in subtropical wetlands: The Everglades. *Environmental Science & Technology*, 42(10), 3494-3500.
32. Rodrigues, D.S., Vieira, L.R., & Silva, F.M. (2022). Phosphorus dynamics in river sediments: A review of source-sink behavior. *Water Research*, 216, 118281. https://doi.org/10.1016/j.watres.2022.118281
33. Santos, R.D., Masaguer, A., & Trasar-Cepeda, C. (2010). Adsorption-desorption of phosphorus in some tropical soils. *Communications in Soil Science and Plant Analysis*, 41(8), 910-923. https://doi.org/10.1080/00103621003680142
34. Sharpley, A.N. and Smith, S.J. (1995). Nitrogen and phosphorus forms in soils receiving manure. *Soil Science*, 159(4), 253-258.
35. Sims, J.R. (1996). Determination of calcium carbonate equivalent in soils using back titration. *Soil Science Society of America Journal*, 60(6), 1577-1583. https://doi.org/10.2136/sssaj1996.03615995006000060025x

36. Smith, V.H., Tilman, G.D. and Nekola, J.C. (1999). Eutrophication: impacts of excess nutrient inputs on freshwater, marine, and terrestrial ecosystems. *Environmental Pollution*, 100(1-3), 179-196.
37. Thomas, G.W. (1962). Exchangeable cations. In C.A. Black (Ed.), *Methods of Soil Analysis, Part 2* (pp. 159-165). American Society of Agronomy.
38. Tiessen, H., & Moir, J. O. (1993). Characterization of available phosphorus by sequential extraction. Soil Science Society of America Journal, 57(3), 1035-1042.
39. Turner, B.L. and Newman, S. (2005). Phosphorus cycling in wetland soils: the importance of phosphate diesters. *Journal of Environmental Quality*, 34(5), 1921-1929.
40. Ulrich, C., & Köhler, S. (2011). Phosphorus is released from sediments of the river Danube. *Science of the Total Environment*, 409(2), 273-280.
41. USEPA. (2008). Nutrient Criteria Technical Guidance Manual: Wetlands. U.S. Environmental Protection Agency, Office of Water, Washington, DC. https://www.epa.gov/nutrientpollution/nutrient-criteria-development-document-wetlands
42. Watson, S.B., Miller, C., Arhonditsis, G., Boyer, G.L., Carmichael, W., Charlton, M.N., Confesor, R., Depew, D.C., Höök, T.O., Ludsin, S.A. and Matisoff, G. (2016). The re-eutrophication of Lake Erie: Harmful algal blooms and hypoxia. *Harmful Algae*, 56, 44-66.
43. Wei, N., Chen, A., Guo, X., Zhang, S., Song, L., Gan, N., Zheng, L., Jia, Y. and Li, J. (2023). Changes in nitrogen metabolism of phosphorus-starved bloom-forming cyanobacterium *Microcystis aeruginosa*: Implications for nutrient management. *Science of the Total Environment*, 903, 166832.
44. Wiegman, A.R., Underwood, K.L., Bowden, W.B., Augustin, I.C., Chin, T. and Roy, E. (2024). Modeling phosphorus retention and release in riparian wetlands restored on historically farmed land. *Journal of Ecological Engineering Design*, 1(1).
45. WWF. (2023). The Ramsar Convention on Wetlands: Not Just for the Birds. *World Wildlife Fund*.
46. **Xu, H., Zou, W., Zhu, G., Qiu, Y., Li, H., Zhu, M., Paerl, H.W., Wu, Z., Qin, B. and Zhang, Y.** (2024). Impoundment-induced stoichiometric imbalance exacerbated phosphorus limitation in a deep subtropical reservoir: implications for eutrophication management. *Water Research*, p.122787.

Figures

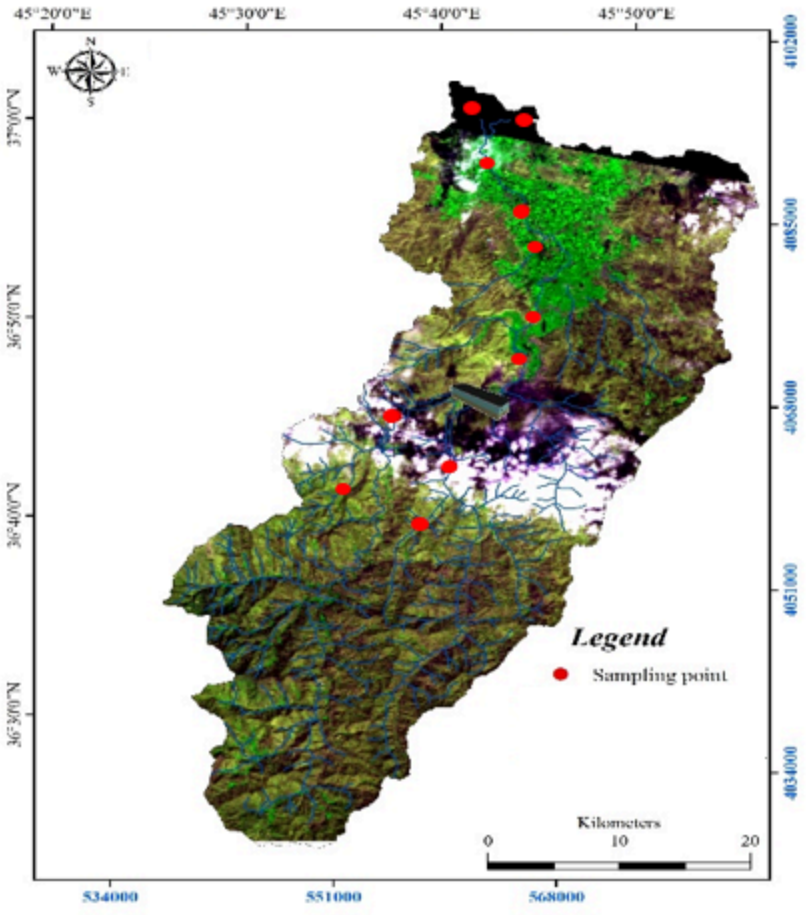


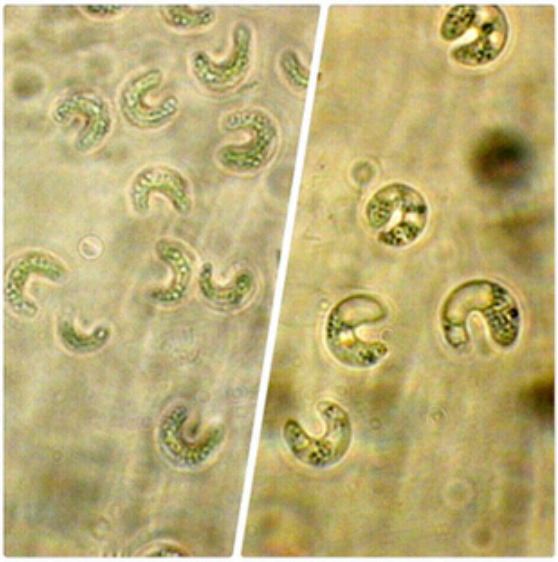
Figure 1

Map of the Mohabad Chai watershed highlighting sediment sampling points. Four upstream sampling points from two tributaries of the Mohabad Chai are indicated, alongside four downstream sediment sampling points. Additionally, two sampling points are shown in the Kani Barazan Wetland located at the downstream site.



Figure 2

Comparison of the water status of the wetland in spring (left image) and summer (right picture). The top photo, taken in spring, shows the wetland in a well-watered state, with extensive water coverage and high water levels, reflecting seasonal precipitation and water influx.



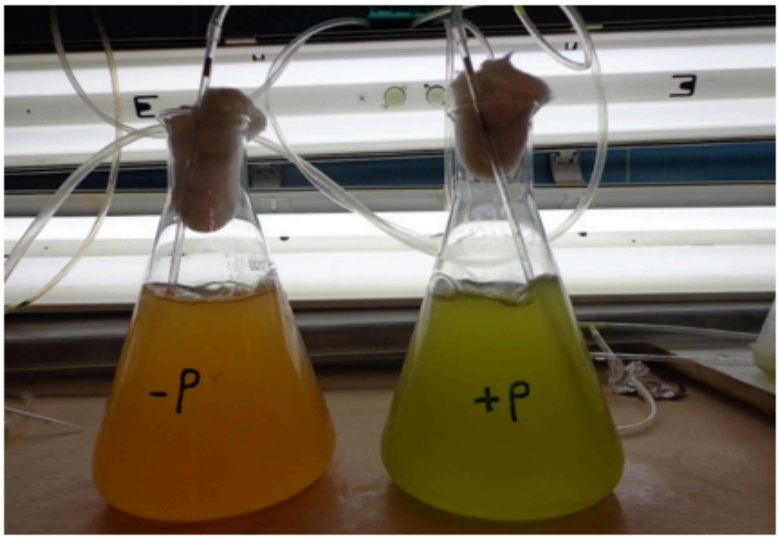


Figure 3

Cultivation of *Raphidocelis subcapitata* under phosphate depletion conditions. (Right) Before phosphate removal (Left) and after phosphate removal (right). Magnification under microscope. (Left) Before phosphate removal (Left) and after phosphate removal (right). The comparison visually represents the morphological changes that can occur in response to nutrient stress, particularly the absence of phosphate.

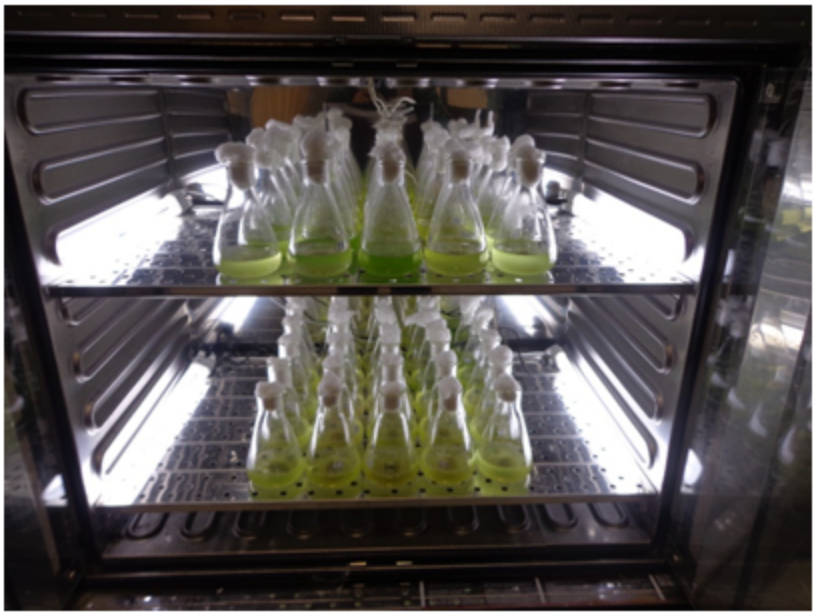


Figure 4

Cultivation of *Selensturm* after the addition of sediments to the culture medium. The image shows the incubator containing multiple Erlenmeyer flasks filled with a phosphorus-free environment (above). The flasks are sealed with a cotton stopper to prevent contamination while allowing gas exchange.

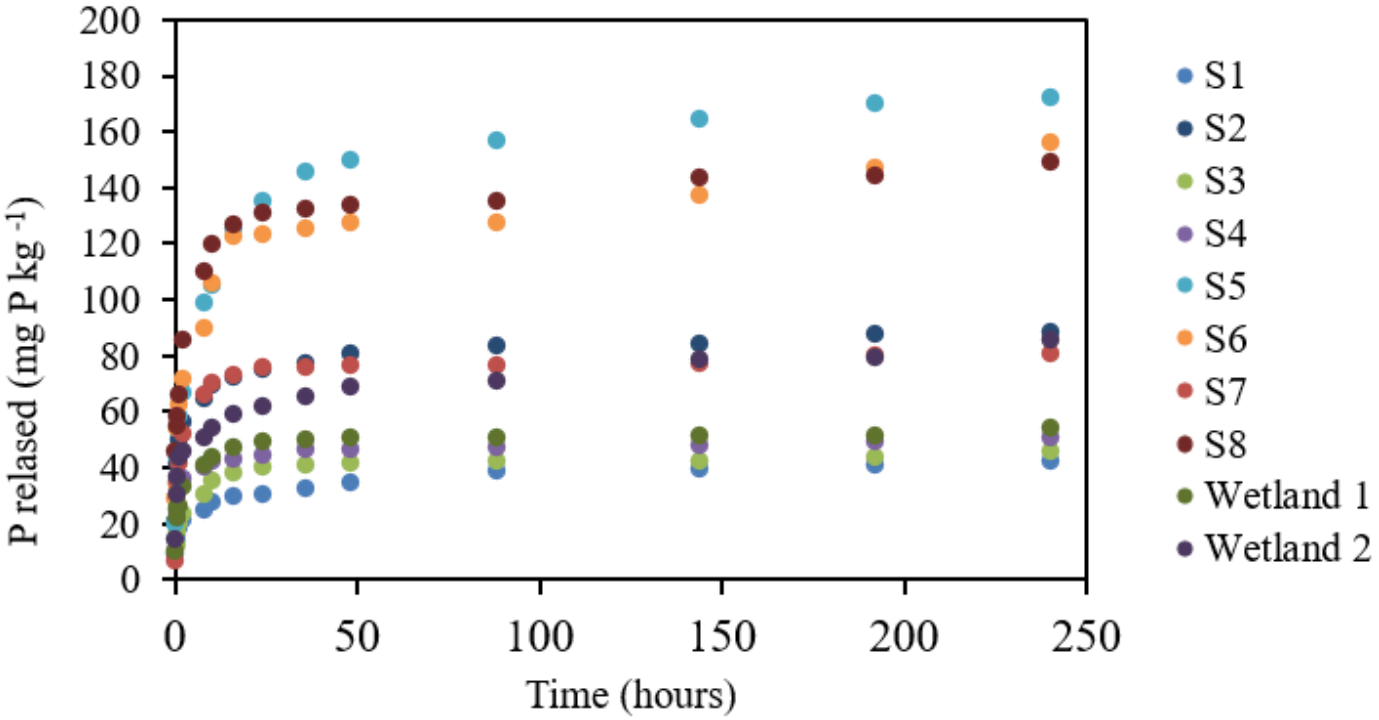


Figure 5

Phosphorus (P) release patterns in sediment samples collected from different locations of the Mohabad River and Kanibarazan Wetland. Sediments S1, S2, S3, and S4 represent downstream sections of the Mohabad River, while S5, S6, S7, and S8 represent upstream sections of the Mohabad River. The two remaining sediments correspond to the Kanibarazan Wetland. The X-axis represents Time (minutes), and the Y-axis shows the Phosphorus concentration (mg L^{-1}) released from sediment samples, highlighting differences in release kinetics and eutrophication potential between river and wetland ecosystems.

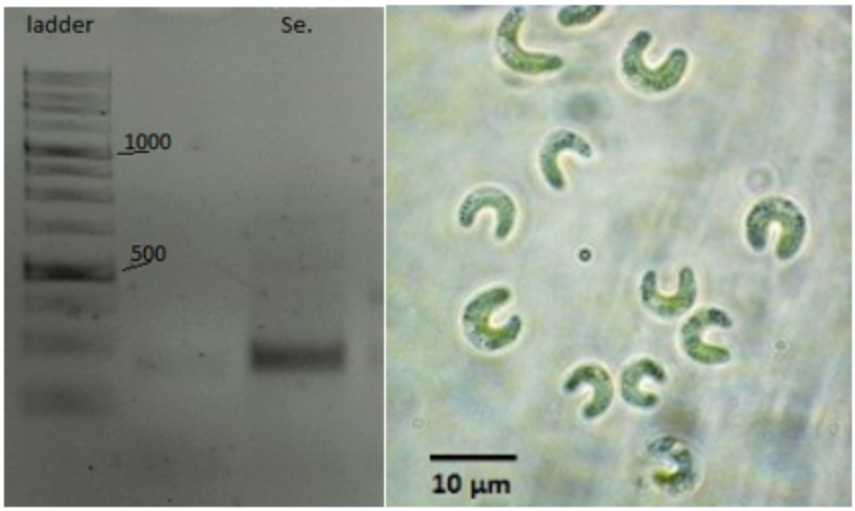


Figure 6

Showcases the distinctive crescent-shaped cells of *Raphidocelis subcapitata* under a microscope (right panel). The left panel presents gel electrophoresis results for the ITS2 region (290 bp). A single, clear band indicates successful amplification of the target DNA sequence. The provided ITS2 sequence (below the figure) further confirms the molecular identity of the isolated algal species.

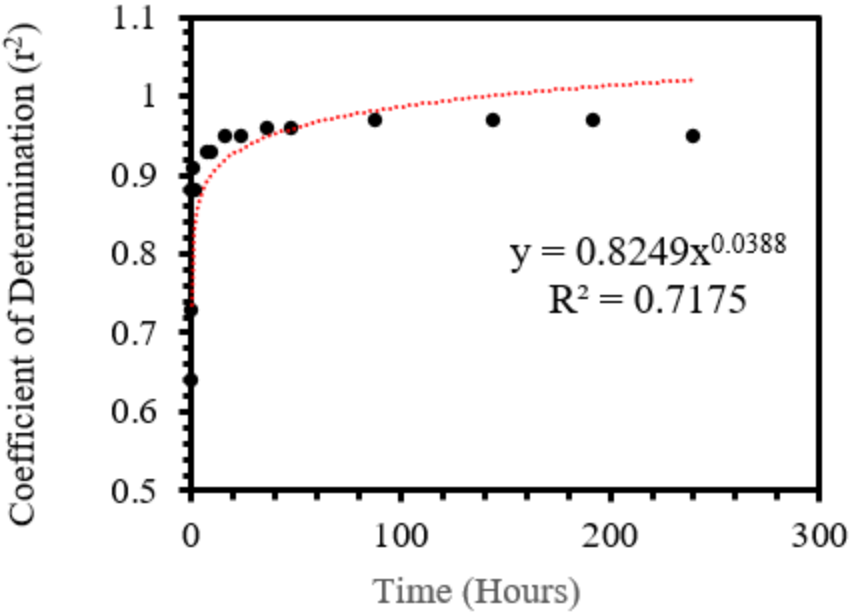


Figure 7

Coefficient of Determination (R^2) for the time-dependent release kinetics of phosphorus (P) in sediment samples over 300 hours. The time (hours) is plotted on the X-axis, while the R^2 values *for Raphidocelis*

subcapitata bioassay response (phosphorus uptake or release correlation) are represented on the Y-axis. The red dotted line indicates the trend of phosphorus release dynamics, showing saturation behavior as time progresses.

		CCE	pH	EC	ACCE	Clay	Sand	KCl-P	NaOH-P	HCl-P	Algal
Parabolic Diffusion	a	-0.38	-0.62	-0.08	-0.54	-0.63	0.62	0.36	0.72	0.01	0.92
	b	-0.33	-0.59	-0.09	-0.46	-0.49	0.39	0.62	0.79	0.02	0.92
Simplified Elovich	a	-0.40	-0.63	-0.11	-0.56	-0.63	0.63	0.39	0.74	-0.01	0.91
	b	-0.34	-0.61	-0.07	-0.46	-0.52	0.41	0.60	0.80	0.03	0.94
Power Function	a	-0.28	-0.35	-0.15	-0.46	-0.59	0.77	-0.09	0.27	-0.09	0.33
	b	-0.23	-0.52	0.04	-0.36	-0.42	0.37	0.52	0.75	0.15	0.95
First order	a	0.23	0.18	0.39	0.22	0.15	-0.13	0.06	-0.01	0.26	0.27
	b	-0.30	0.26	0.07	-0.42	-0.62	0.51	0.26	0.74	0.12	0.90
Second order	a	0.30	0.67	-0.11	0.35	0.67	-0.34	-0.15	-0.69	-0.12	-0.74
	b	0.01	0.26	-0.33	0.10	0.21	-0.27	-0.26	-0.57	-0.30	-0.86

Figure 8

Figure 7. Correlation coefficients of physicochemical soil properties (CCE, pH, EC, ACCE, clay, and sand) and phosphorus fractions (KCl-P, NaOH-P, and HCl-P) with algal growth under various kinetic models (Parabolic Diffusion, Elovich, Power, First-order, and Second order). Positive and negative correlations are observed across models, with algal growth showing strong relationships (e.g., 0.92–0.95) under the Parabolic, Elovich, and Power models. At the same time, phosphorus fractions exhibit variable trends depending on the model and soil properties.